Am J Transl Res 2026;18(9):8350-8363
www.ajtr.org /ISSN:1943-8141/AJTR0173207

Original Article

Exosomes derived from induced pluripotent stem cells can repair cartilage damage after arthroscopic microfracture surgery by delivering microRNA-140-3p

Haiming Wang*, Caiqi Xu*, Chen Chen

*Department of Orthopaedic Surgery, Shanghai Sixth People's Hospital, Shanghai, China. *Co-first authors.*

Received April 10, 2026; Accepted August 11, 2026; Epub September 15, 2026; Published September 30, 2026

Abstract: Objective: To investigate whether induced pluripotent stem cell-derived exosomes (iExos) can repair cartilage damage after arthroscopic microfracture (MF) surgery by delivering microRNA (miR)-140-3p. Methods: iExos were extracted via ultracentrifugation. Bone marrow mesenchymal stem cells (BMSCs) were divided into control, iExos, negative control, and miR-140-3p inhibitor groups. Chondrogenic and hypertrophic markers were assessed. Forty Sprague-Dawley rats were randomized into control, sham, MF, and MF+iExos groups. Cartilage repair was evaluated by behavioral, biomechanical, histological, and immunohistochemical analyses. Results: In vitro, iExos upregulated chondrogenic markers (SOX9, COL2A1, ACAN) and downregulated hypertrophic markers (collagen type X alpha 1 chain, MMP13, RUNX2) in BMSCs (P<0.05), effects reversed by miR-140-3p inhibition (P<0.05). In vivo, the MF+iExos group showed improved gait parameters, joint range of motion, International Cartilage Regeneration and Joint Preservation Society gross score, elastic modulus, and relaxation modulus versus MF group (P<0.05), reaching near-sham levels. Histologically, the MF+iExos group exhibited thicker, smoother repair tissue, lower Mankin score, and higher glycosaminoglycan content (P<0.05). Immunohistochemistry revealed increased type II collagen (COL2) expression, decreased type I collagen (COL1) expression, and a higher COL2/COL1 ratio (P<0.05), also restored to near-sham levels. Conclusion: iExos promote chondrogenic differentiation of BMSCs and inhibit hypertrophy via miR-140-3p delivery, effectively repairing cartilage damage after arthroscopic MF, offering a novel therapeutic strategy for cartilage repair.

Keywords: Induced pluripotent stem cells, MicroRNA-140-3p, induced pluripotent stem cell-derived exosomes, microfracture, articular cartilage defect

Introduction

Articular cartilage injury is a common disease seen in sports medicine and orthopedics, often causing joint pain, functional impairment, and it can eventually develop into osteoarthritis, significantly affecting the quality of life of patients [1]. Due to the limited self-repairing capacity of joints, once full-thickness defects occur, spontaneous regeneration is difficult to achieve [2]. Arthroscopic microfracture (MF) surgery, is a method for treating injuries by inducing fibrocartilage repair [3, 4]. However, the fibrocartilage formed after MF surgery has much poorer biomechanical properties and wear resistance than native hyaline cartilage. Long-term follow-up results show that it carries a risk of degeneration and often fails to completely repair the defect area, limiting its application effect in young or highly active patients [5, 6]. Therefore, exploring how to optimize the repair microenvironment after MF surgery, promoting the differentiation of bone marrow mesenchymal stem cells (BMSCs) into hyaline cartilage and inhibiting their hypertrophy, has become a key issue in the regeneration of articular cartilage.

Exosomes, as an important medium for intercellular communication, have attracted increasing research attention in recent years. Exosomes can regulate the functions of target cells by targeted delivery of bioactive molecules [7]. Exosomes derived from stem cells have similar repair capabilities as the parent cells, which makes them ideal carriers for cell-free

https://doi.org/10.62347/LNQN2685

therapeutic strategies [8]. In particular, induced pluripotent stem cells (iPSCs) possess self-renewal capacity and are not constrained by ethical concerns; accordingly, iPSC-derived exosomes (iExos) have attracted considerable attention in promoting tissue repair [9]. In the process of cartilage development and homeostasis maintenance, microRNAs (miRNAs) play a crucial regulatory role. Among them, miRNA (miR)-140-3p is one of the miRNAs in the cartilage tissue, directly participating in the regulation of the balance between cartilage formation and degradation [10]. Studies have shown that miR-140-3p can promote the expression of chondrogenic markers by targeting genes such as histone deacetylase 4 (HDAC4), while inhibiting the expression of hypertrophic-related factors, thereby maintaining the phenotype of chondrocytes and inhibiting the progression of osteoarthritis [11]. However, the simple delivery of miRNAs has problems such as instability in vivo and poor targeting. Utilizing stem cell exosomes can efficiently deliver miR-140-3p to BMSCs at the damaged site may be an effective strategy to enhance the quality of cartilage repair after MF.

Based on this background, this study established a rat model of cartilage injury after MF surgery, and combined cell-level experiments to systematically investigate the regulatory effect of iPSCs-derived iExos in delivering miR-140-3p to promote the chondrogenic differentiation of BMSCs. The aim is to provide a new theoretical basis and potential cell-free therapeutic strategies for the treatment of cartilage injury after MF surgery in clinical practice.

Materials and methods

Cell source, culture and processing

Cultivation of iPSCs: Human iPSCs were purchased from the Stem Cell Bank of the Chinese Academy of Sciences (lot No. SCSP-305). The cells were cultured in mTeSR1 medium (STEMCELL Technologies, Canada, lot No. 85850) and placed in a cell culture incubator at 37°C and 5% CO_2 (Thermo Fisher Scientific, USA, Model 3111). When cells reached 80% confluence, passage was performed using 0.5 mM ethylenediaminetetraacetic acid (EDTA) (Invitrogen, USA, cat. No. 15575-038).

Chondrogenic differentiation of iPSCs: iPSCs were cultured in a three-dimensional microsphere method. The cells were seeded at a density of 2.5×10^5 cells per sphere onto low-adhesion 96-well plates (Corning, USA, cat. No. CLS7007). The cells were cultured in chondrogenic induction medium (Gibco, USA, cat. No. 11965092) supplemented with 1% insulin-transferrin-selenium (BD Biosciences, USA, cat. No. 354352), 100 nM dexamethasone (Sigma-Aldrich, USA, cat. No. D4902), 10 ng/mL TGF-β3 (PeproTech, USA, cat. No. 100-36E) for 21 days.

Exosome extraction: The supernatant of iPSCs cultured under chondrogenic differentiation conditions for 21 days was collected. Exosomes were isolated by differential ultracentrifugation. All centrifugation steps were performed at 4°C. Briefly, the cell culture supernatant was collected and centrifuged at 300×g for 10 min to remove cells, followed by 2,000×g for 20 min to remove cell debris, and then 10,000×g for 30 min to remove large extracellular vesicles. The resulting supernatant was filtered through a 0.22-μm pore filter (Millipore, USA) and then ultracentrifuged at 100,000×g for 70 min (Beckman Coulter, Optima XE-90, rotor Type 70 Ti) to pellet the exosomes. The pellet was washed with phosphate-buffered saline (PBS) and re-ultracentrifuged at 100,000×g for 70 min. The final exosome pellet was resuspended in sterile PBS and stored at -80°C until use. All ultracentrifugation steps were carried out at 4°C. The supernatant of iPSCs without chondrocyte differentiation induction was extracted for exosomes using the same method as a negative control (iExos-NC; exosomes from non-induced iPSCs). Transmission electron microscopy, Western blotting for exosomal markers (CD63, TSG101, and Alix), and nanoparticle tracking analysis were performed to characterize the isolated exosomes (Supplementary Figure 2). The quantitative reverse transcription polymerase chain reaction (qRT-PCR) results showed that, compared with iExos-NC (P= 0.0004) and the parental iPSCs (P=0.00011), the level of miR-140-3p in iExos was significantly increased. These results confirm that after iPSCs undergo chondrogenic induction, miR-140-3p was specifically enriched in the secreted exosomes. See Supplementary Figure 1A.

Isolation and culture of BMSCs: After the male Sprague-Dawley (SD) rats (weighing 80-100 g, purchased from Beijing Vitogen Life Sciences Co., Ltd.) were sacrificed, the femurs and tibias were isolated under aseptic conditions. The epiphyseal ends were cut off, and the bone marrow cavities were repeatedly rinsed with Dulbecco's Modified Eagle Medium/Ham's F-12 Nutrient Mixture (Gibco, USA, cat. No. 11320033) containing 10% fetal bovine serum and 1% penicillin-streptomycin (cat. No. 15140122). The collected cells were filtered through a 200-mesh filter and centrifuged (300×g, 5 min) before being resuspended in complete medium and culturing in a 37°C, 5% CO_2 incubator. The medium was changed after 48 hours, removing the non-adherent cells. When cells reached 80% confluence, 0.25% trypsin-EDTA (Gibco, USA, cat. No. 25200072) was used to digest and passage the cells. The qRT-PCR results showed that compared with the iExos-NC group (P=0.00026), the level of miR-140-3p in BMSCs after iExos treatment was significantly increased, indicating that iExos can effectively deliver miR-140-3p to the receptor BMSCs (Supplementary Figure 1B).

Chondrogenic induction group of BMSCs: When cells reached 80% confluence, the medium was replaced with chondrogenic induction medium (Dulbecco's Modified Eagle medium, same as above). Cells were divided into the following four groups and cultured for 21 days: (1) Control group (routine culture); (2) iExos group (chondrogenic induction medium supplemented with 80 μg/mL iExos); (3) iExos-NC group (chondrogenic induction medium supplemented with 80 μg/mL iExos-NC); and (4) miR-140-3p inhibitor group (chondrogenic induction medium supplemented with 80 μg/mL iExos and 50 nM miR-140-3p inhibitor; RiboBio, Guangzhou, China, cat. No. miR200-00131-1-5). The corresponding treatments were freshly prepared and added to the culture medium at each medium change (every 3 days) throughout the 21-day culture period.

Animal sources and grouping

Experimental animals and ethics: Specific pathogen-free male SD rats, 12-16 weeks old, weighing 300-400 g, were purchased from Beijing Vitogen Laboratory Animal Technology Co., Ltd. (License No. SCXK (Beijing) 2024-0008). All animals were housed in a constant temperature (22±2°C), constant humidity (50%±10%), 12-hour light/12-hour dark cycle environment. The experimental protocol was approved by the Experimental Animal Ethics Committee of the Chinese People's Liberation Army General Hospital (2024-012-01).

Animal grouping: Forty SD rats were randomly divided into four groups using a random number table: (1) control group (untreated); (2) sham group (joint cavity opened without defect creation); (3) MF group (cartilage defect+ MF surgery); and (4) MF+iExos group (cartilage defect + MF surgery + local injection of 50 μL iExos at 100 μg/mL immediately after surgery) [12]. To account for potential uncontrollable factors (e.g., postoperative infection and sample processing failure) and the different requirements of various destructive tests, the initial sample size was set at 10 rats per group. At 12 weeks post-surgery, following euthanasia, six rats from each group were randomly selected for biomechanical testing, and histological and immunohistochemical analysis. The remaining samples were reserved as backups in case of processing failures.

Arthroscopic MF surgery modeling

Rats were anesthetized by intraperitoneal injection of 3% pentobarbital sodium (Sigma-Aldrich, USA, cat. No. P3761) at a dose of 40 mg/kg. They were placed in a supine position and prepared and disinfected. A parapatellar incision was made on the inner side of the knee joint, and under the assistance of the arthroscopic system (Karl Storz, Germany, 30° arthroscopy), the intercondylar fossa of the femur was exposed. A full-thickness cartilage defect reaching the subchondral bone was created using a micro-bone drill (diameter 0.8 mm, Stryker, USA) on the femoral condyle. Then, a 1.0-mm Kirschner wire was inserted into the subchondral bone until fat droplets exuded. The sham surgery group only opened the joint cavity without creating the defect or performing MF treatment. The MF+iExos group immediately injected 50 μL of exosome suspension (concentration 100 μg/mL, containing miR-140-3p) at the defect site after MF, while the MF group injected the same volume of PBS. The rats were housed in individual

Table 1. Quantitative PCR primer sequences

Gene name	Forward primer (5'-3')	Reverse primer (3'-5')
SOX9	GGCAAGCTCTGGAGACTTCTG	CCCGTTCTTCACCGACTTCC
COL2A1	AAGGATGGCTGCACGAAACA	TGTCCATGGGTGCAATGTCAA
ACAN	ACACTGGCGAGCACTGTAAC	GCTGGGAAGGCATAAGCATGT
COLX	GAGATGCATTTGGAGGTAGG	GATTGCTGAGTGCTCCGGAG
MMP13	AACCAGATGTGGAGTGCCTGATG	CACATCAGACCAGACCTTGAAGGC
RUNX2	CCACCACTCACTACCACACG	GGACGCTGACGAAGTACCAT
GAPDH	CCTCTGACTTCAACAGCGACA	GTTGTCATACCAGGAAATGAGCTTG

Note: PCR, polymerase chain reaction; SOX9, SRY-box transcription factor 9; COL2A1, collagen type II alpha 1 chain; ACAN, aggrecan; COLX, collagen type X alpha 1 chain; MMP13, matrix metallopeptidase 13; RUNX2, runt-related transcription factor 2; GAPDH, glyceraldehyde-3-phosphate dehydrogenase.

cages and allowed free movement after the surgery.

Western blot analysis

After 21 days of chondrogenic induction of BMSCs, cells were washed twice with cold PBS and lysed with radioimmunoprecipitation assay lysis buffer (Beyotime, cat. No. P0013B) containing protease and phosphatase inhibitors on ice for 30 min. The lysates were centrifuged at 12,000×g for 15 min at 4°C, and the supernatants were collected. Protein concentrations were determined using a bicinchoninic acid assay. Equal amounts of protein (20 μg per lane) were separated by sodium dodecyl sulfate-polyacrylamide gel electrophoresis and transferred onto polyvinylidene difluoride membranes (Millipore, cat. No. IPVH00010). The membranes were incubated overnight at 4°C with primary antibodies against SRY-box transcription factor 9 (SOX9; cat. No. ab185230; 1:1000), collagen type II alpha 1 chain (COL2A1; cat. No. ab34712; 1:1000), aggrecan (ACAN; cat. No. ab36896; 1:1000), collagen type X alpha 1 chain (COLX; cat. No. ab58632; 1:1000), matrix metallopeptidase 13 (MMP13; cat. No. ab39012; 1:1000), runt-related transcription factor 2 (RUNX2; cat. No. ab23981; 1:1000), and β-actin (cat. No. ab8226; 1:2000; all from Abcam, UK). After washing, the membranes were incubated with horseradish peroxidase-conjugated secondary antibody (1:5000; cat. No. ab205718; Abcam, UK) at room temperature for 1 hour. Protein bands were visualized using an enhanced chemiluminescence luminescent reagent (Millipore, USA, cat. No. WBKLS0500).

qRT-PCR

The RNA concentration and purity were detected using NanoDrop 2000 (Thermo Fisher Scientific, USA). Reverse transcription was performed according to the manufacturer's instructions for PrimeScrip RT Master Mix (TaKaRa, Japan, cat. No. RR036A), with reaction conditions of 37°C for 15 min and 85°C for 5 s. Quantitative PCR was conducted using TB Green Premix Ex Taq II (TaKaRa, Japan, cat. No. RR820A) on the QuantStudio 5 Real-Time PCR System (Applied Biosystems, USA), with reaction conditions: initial denaturation at 95°C for 30 s, followed by 40 cycles of 95°C for 5 s and 60°C for 34 s. Glyceraldehyde-3-phosphate dehydrogenase was used as the internal reference, and the relative expression of the target gene was calculated using the $2^{-\Delta\Delta Ct}$ method. The primer sequences are shown in **Table 1**.

Behavioral observation

At 4, 8, and 12 weeks post-surgery, gait analysis was conducted using the CatWalk gait analysis system [13], and hindlimb gait parameters, including stand time, swing time, and stride length, were recorded. At the same time, joint range of motion was evaluated using a joint mobility score. Two independent researchers blinded to the grouping passively flexed and extended the rats' knees, and the range of motion was graded on a scale of 0 to 3 (0, free movement; 1, mild restriction; 2, moderate restriction; 3, severe restriction). The average of the two scores was used as the final score.

Animal euthanasia and sample collection

At 12 weeks post-surgery, all rats were deeply anesthetized by intraperitoneal injection of 3% pentobarbital sodium at a dose of 100 mg/kg. After confirming loss of the pedal and corneal reflexes, euthanasia was performed by intraperitoneal injection of an overdose of pentobarbital sodium (200 mg/kg). Death was confirmed by cessation of heartbeat and respiration for at least 5 min, as well as absence of response to toe pinch. The incision was reopened along the original surgical site, and the knee joint was exposed. The hindlimb and knee joint tissues were harvested. The joint surface repair was observed under a stereomicroscope, and the International Cartilage Regeneration and Joint Preservation Society (ICRS) gross score was assessed. Specimens of the distal femur and proximal tibia were fixed in 4% paraformaldehyde (Biosharp, China, cat. No. BL539A) for 48 hours, then decalcified in 10% EDTA solution (Sigma-Aldrich, USA, cat. No. E6758) for 3 weeks. The decalcification solution was changed every 3 days.

Biomechanical testing and histological scoring

Samples were harvested from the repaired cartilage areas of the distal femur in each group. Samples were cut into cylindrical specimens (3 × 3 × 2 mm; n=6 per group). The specimens were tested using a dynamic mechanical analyzer. Before testing, the specimens were immersed in PBS for 30 min to equilibrate. The test parameters were as follows: compression mode, preload 0.1 N, frequency 1 Hz, and temperature 25°C. The elastic modulus and relaxation modulus were recorded.

Two independent researchers blinded to the grouping assessed the femoral condyle cartilage defects using the ICRS gross scoring criteria [14]. The scoring criteria included defect repair, integration with surrounding cartilage, and surface architecture of the repaired tissue.

Histological and immunohistochemical analysis

Tissue embedding and sectioning: After decalcification, the specimens were dehydrated with graded ethanol and embedded in paraffin (Leica, Germany, EG1150H). Serial coronal sections were cut at a thickness of 4 μm, adhered to anti-drying slides (Thermo Fisher Scientific, USA, cat. No. 4951PLUS4), and left to dry at 60°C for 2 hours before being stored.

Hematoxylin-eosin (HE) staining: The sections were deparaffinized to water. The tissue was stained with hematoxylin (Beijing Zhongshan Jinqiao, cat. No. ZLI-9610), followed by eosin (Wuhan Saiwei, cat. No. G1002) for 1 min, dehydrated with gradient ethanol, cleared, and the cartilage repair tissue was observed under a light microscope (Olympus BX53, Japan). A semi-quantitative assessment of the degree of cartilage degeneration was performed using the Mankin scoring system [15]. This scoring system evaluates from four aspects: (1) tissue structure (0-3 points); (2) cell number and distribution (0-3 points); (3) matrix staining with toluidine blue or safranin O (0-3 points); and (4) integrity of the marginal line (0-1 point), with a total score ranging from 0 to 14 points. A higher score indicates more severe cartilage degeneration. To ensure objectivity and reproducibility, all sections were independently evaluated and scored by two pathologists with ten years of experience who were blinded to the experimental groups. The average score of the two was taken as the final statistical value.

Scarlet O and quin green staining: After the section was deparaffinized to water, it was immersed in quin green staining solution (Sival, China, cat. No. G1285) for 5 min. Excess staining solution was washed off with acetic acid, and then the section was stained with Scarlet O staining solution (Sival, China, cat. No. G1285) for 3 min. It was then rapidly dehydrated, cleared, and sealed. The positive area of Scarlet O staining was analyzed using ImageJ software (NIH, USA) to calculate the relative glycosaminoglycan (GAG) content.

Immunohistochemical staining: The sections were deparaffinized to water and incubated with 3% H_2O_2 for 10 min. Antigen retrieval was performed using sodium citrate buffer (Zhongshan Golden Bridge, China) in a microwave oven for 10 min, and then the sections were blocked with 10% goat serum for 30 min. Primary antibodies were added: rabbit anti-rat COL2A1 antibody (1:200, Abcam, UK, cat. No. ab34712) and rabbit anti-rat collagen type I alpha 1 chain antibody (1:200, Abcam, UK, cat.

No. ab260043). The samples were incubated at 4°C overnight. Then, horseradish peroxidase-labeled goat anti-rabbit secondary antibody (1:500, Abcam, UK, cat. No. ab205718) was added for 30 min. 3,3'-diaminobenzidine staining (Beyotime, China, cat. No. P0203), hematoxylin counterstaining, dehydration and mounting were performed. The positive staining integral optical density was analyzed using ImageJ software, and the type II collagen/type I collagen (COL2/COL1) ratio was calculated.

Statistical analysis

Statistical analyses were performed using Statistical Package for the Social Sciences 27.0.1 (IBM, USA). The Shapiro-Wilk test was used to assess data normality, and Levene's test was used to assess homogeneity of variances. Normally distributed continuous variables are reported as mean ± standard deviation; non-normally distributed variables are reported as median (interquartile range). One-way analysis of variance was used for comparisons among multiple groups, and independent-samples t-tests were used for two-group comparisons, when data met normality and homogeneity of variance assumptions. For data that violated normality or homogeneity of variance, the Kruskal-Wallis test was used for multiple groups, and the Mann-Whitney U test was used for two-group comparisons. All experiments were independently repeated at least three times. Statistical significance was defined as $P<0.05$.

Results

iExos promotes chondrogenesis of BMSCs and inhibits hypertrophy in vitro through miR-140-3p

To verify the regulatory effect of iExos on the differentiation direction of BMSCs, we examined the expression of chondrogenic markers (SOX9, COL2A1, ACAN) and hypertrophic markers (COLX, MMP13, RUNX2). Compared with the control group, the protein and mRNA levels of chondrogenic markers in BMSCs treated with iExos were significantly increased (SOX9, $P=0.0002$; COL2A1, $P=0.0001$; ACAN, $P=0.0003$), while the levels of hypertrophic markers were significantly decreased (COLX, $P=0.0004$; MMP13, $P=0.0005$; RUNX2, $P=0.0006$). In contrast, no significant differences were observed between the iExos-NC group and the control group (all $P>0.05$). Furthermore, when the miR-140-3p inhibitor was added together with iExos, the above chondrogenic effects were significantly reversed, as evidenced by decreased chondrogenic marker expression and increased hypertrophic marker expression (all $P<0.05$), indicating that the function of iExos depends on the delivery of miR-140-3p (**Figure 1**).

Intra-articular injection of iExos significantly improves joint function in rats after MF surgery

Postoperative functional recovery was evaluated using CatWalk gait analysis and joint range of motion scoring. At 12 weeks post-surgery, compared with the sham group, standing time ($P=0.00015$) and stride length ($P=0.0008$) were significantly decreased in the MF group, whereas the joint range of motion score ($P=0.0003$) and swing time ($P=0.0004$) were significantly increased. Moreover, standing time ($P=0.00017$), and stride length ($P=0.00012$) were significantly improved in the MF+iExos group compared with the MF group, whereas swing time ($P=0.0009$) and joint range of motion score ($P=0.0006$) were significantly decreased, reaching levels comparable to those in the sham group (**Figure 2**).

iExos improves the biomechanical properties and gross appearance scores of repaired cartilage

The ICRS gross scores and biomechanical test results showed that the ICRS gross score (median 4.00), elastic modulus (2.91±0.11 MPa), and relaxation modulus (1.38±0.08 MPa) in the MF group were significantly lower than those in the sham group (all $P<0.001$). All these parameter were significantly improved in the MF+iExos group: the ICRS gross score increased to 10.00 ($P=0.00001$ vs. MF group), the elastic modulus increased to 7.23±0.15 MPa ($P<0.001$), and the relaxation modulus increased to 3.57±0.11 MPa ($P<0.001$), indicating that iExos-treated repair tissue acquired mechanical properties closer to those of native cartilage (**Table 2**).

iExos improves the structural integrity and extracellular matrix quality of repaired tissue

HE staining showed that the repaired tissue in the MF group had a rough surface and disordered structure, with a Mankin score of

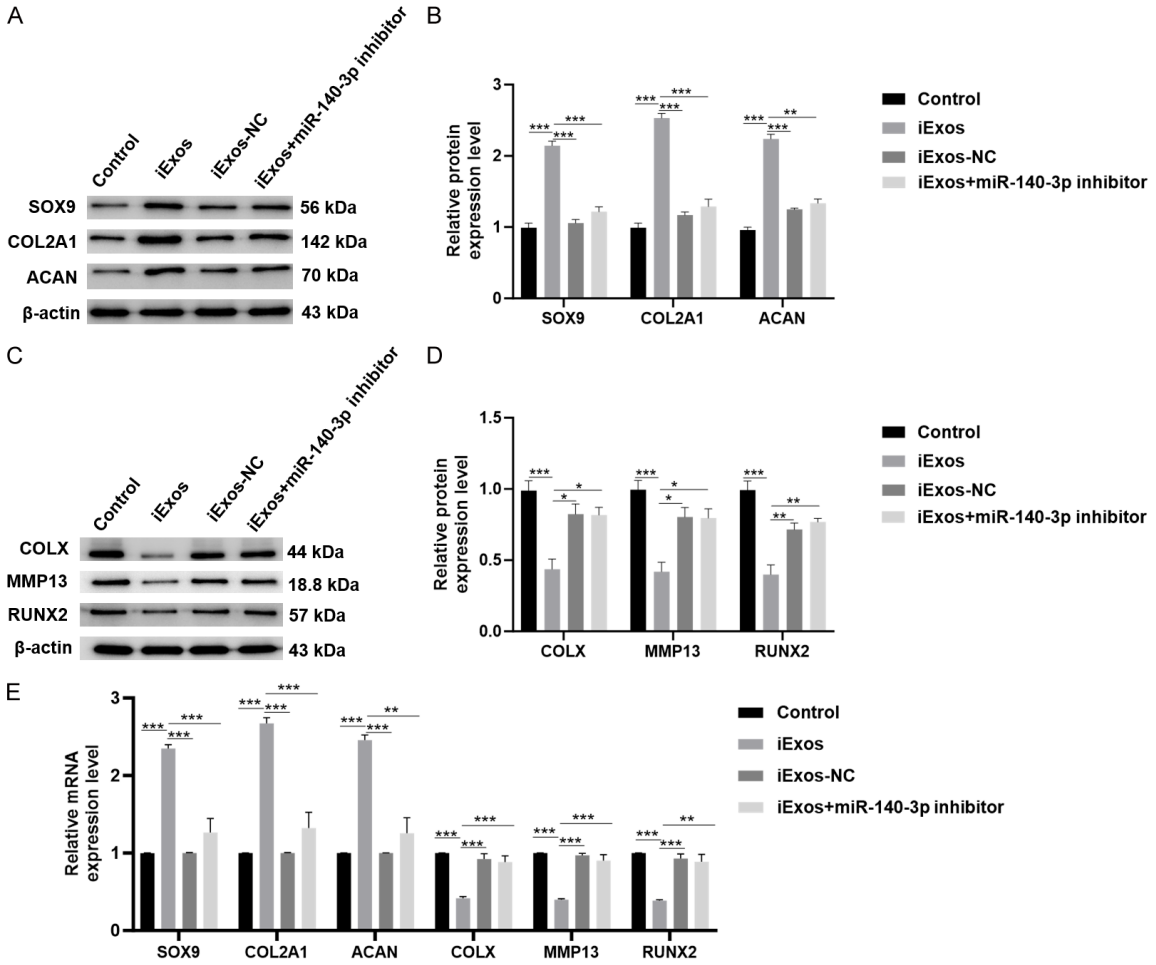


Figure 1. Chondrogenic and hypertrophic marker expression. A. Protein expression of SOX9, COL2A1, ACAN, and β-actin in BMSCs. B. Quantification of SOX9, COL2A1, and ACAN protein expression in BMSCs. C. Protein expression of COLX, MMP13, RUNX2, and β-actin in BMSCs. D. Quantification of COLX, MMP13, and RUNX2 protein expression in BMSCs. E. mRNA expression levels of SOX9, COL2A1, ACAN, COLX, MMP13, and RUNX2 in BMSCs. $^{***}P<0.001$; $^{**}P<0.01$; $^{*}P<0.05$. n=3 per group. Abbreviations: BMSCs, bone marrow mesenchymal stem cells; SOX9, SRY-box transcription factor 9; COL2A1, collagen type II alpha 1 chain; ACAN, aggrecan; COLX, collagen type X alpha 1 chain; MMP13, matrix metallopeptidase 13; RUNX2, runt-related transcription factor 2; β-actin, beta-actin; miR/mRNA, microRNA; iExos, induced pluripotent stem cell-derived exosomes; iExos-NC, exosomes from non-induced induced pluripotent stem cells.

(9.5±1.0), which was significantly higher than that of the sham group ($P<0.001$). The repaired tissue in the MF+iExos group was thicker, smoother, and the cell arrangement was more dense, with a Mankin score of (4.2±0.8), which was significantly lower than that of the MF group ($P=0.00024$) (**Figure 3**). Periodic acid-Schiff staining showed that the GAG content in the MF group was significantly lower than that in the sham group ($P=0.000015$), while the GAG content in the MF+iExos group significantly increased ($P=0.00018$ vs. MF group), approaching the level of the sham group (**Figure 4**).

iExos promotes a hyaline cartilage-specific collagen phenotype

Immunohistochemical staining showed that in the joint cartilage of the sham and the control groups, COL2 was highly expressed, whereas COL1 was barely expressed. In the MF group, COL1 was highly expressed and COL2 was weakly expressed, and the COL2/COL1 ratio was significantly decreased ($P=0.000022$ vs. sham group). In contrast, in the MF+iExos group, COL2 expression was significantly increased, whereas COL1 expression was decreased, and the COL2/COL1 ratio was sig-

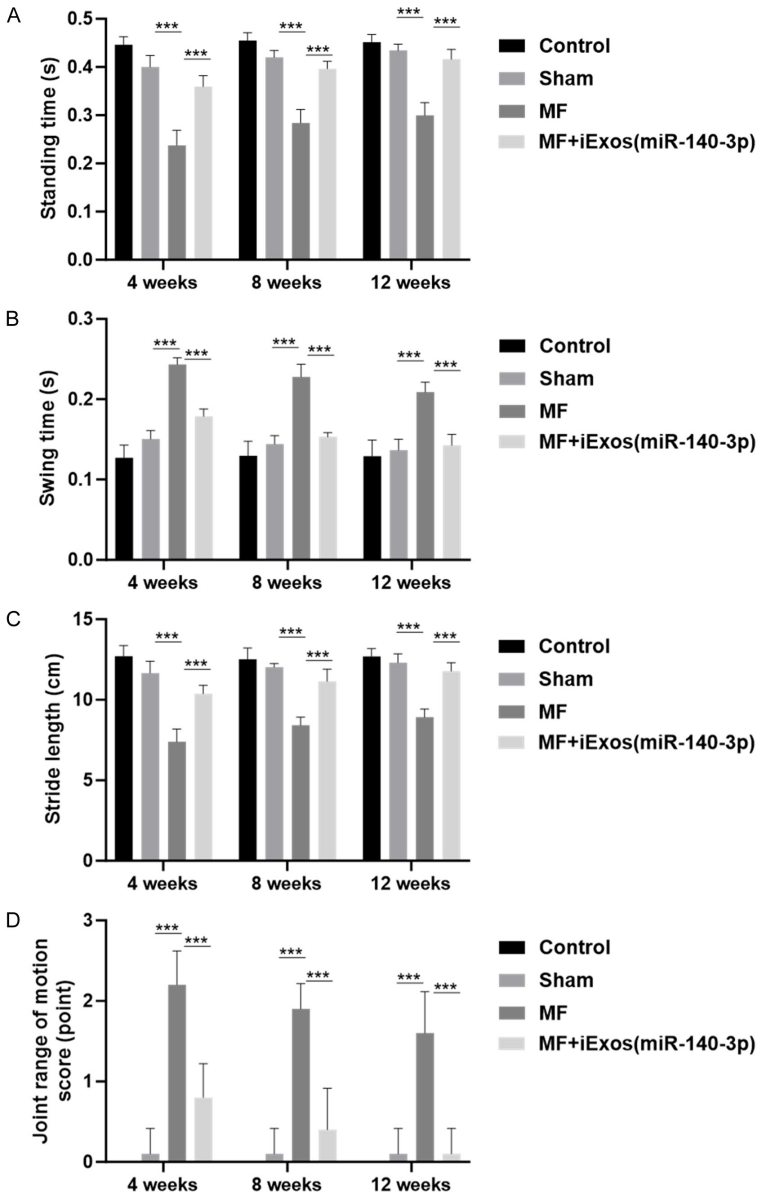


Figure 2. Behavioral observation parameters. (A-C) Standing time, swing time, and stride length in the four groups at 4, 8, and 12 weeks post-surgery. (D) Joint range of motion scores in the four groups at 4, 8, and 12 weeks post-surgery (Since the control group is normal, the score value is 0, so the bar chart is not shown in (D). ***P<0.001. n=10 per group. Abbreviations: MF, microfracture; iExos, induced pluripotent stem cell-derived exosomes; miR, microRNA.

nificantly higher than that of the MF group (P=0.00009), reaching a level comparable to that of the sham group (**Figure 5**).

Discussion

The repair of joint cartilage damage remains a major challenge in both sports medicine and regenerative medicine [16, 17]. MF is currently the clinical treatment for cartilage defects; however, the fibrous cartilage it generates is markedly inferior in both mechanical properties and tissue structure when compared with native hyaline cartilage, leading to limited long-term efficacy [16, 17]. In recent years, a cell-free therapeutic strategy based on iExos to has been used to optimize the post-MF repair microenvironment. This strategy harnesses the regenerative efficacy of stem cells while offering the advantage of low immunogenicity [18]. In the present study, we demonstrated that iExos can effectively deliver miR-140-3p, thereby inducing chondrogenic differentiation of BMSCs in vitro and concurrently suppressing their hypertrophic differentiation. In vivo, treatment with iExos improved the gait function, joint range of motion, quality of the repaired cartilage tissue, and biomechanical properties of rats following MF surgery, ultimately restoring these parameters to near-normal levels.

During cartilage tissue formation, the ultimate nature of the repaired tissue is largely governed by the equilibrium between chondrocyte differentiation and the subsequent process of hypertrophy [19]. SOX9 serves as a master transcription factor that preserves the chondrocytic phenotype, and it is capable of driving the expression of pro-chondrogenic genes, including COL2A1 and ACAN [20]. In contrast, markers such as COLX, MMP13, and RUNX2 are characteristic of chondrocyte hypertrophy and terminal differentiation. Elevated expression of these factors is typically associated with the formation of fibrocartilage or the development of osteoar-

Table 2. ICRS gross score and biomechanical testing

	Control (n=6)	Sham (n=6)	MF (n=6)	MF+iExos (n=6)	*H/F*	*P*
ICRS score (score)	12.00 (11.00, 12.00)	12.00 (11.00, 12.00)	4.00 (3.00, 5.00)[a]	10.00 (9.00, 10.25)[b]	19.699	<0.001
Elastic modulus (MPa)	8.63±0.13	8.49±0.09	2.91±0.11[a]	7.23±0.15[b]	51.600	<0.001
Relaxation modulus (MPa)	4.30±0.09	4.18±0.08	1.38±0.08[a]	3.57±0.11[b]	32.190	<0.001

Note: Compared with the sham group, [a]*P*<0.001; compared with the MF group, [b]*P*<0.001. Abbreviations: ICRS, International Cartilage Regeneration and Joint Preservation Society; MF, microfracture; iExos, induced pluripotent stem cell-derived exosomes.

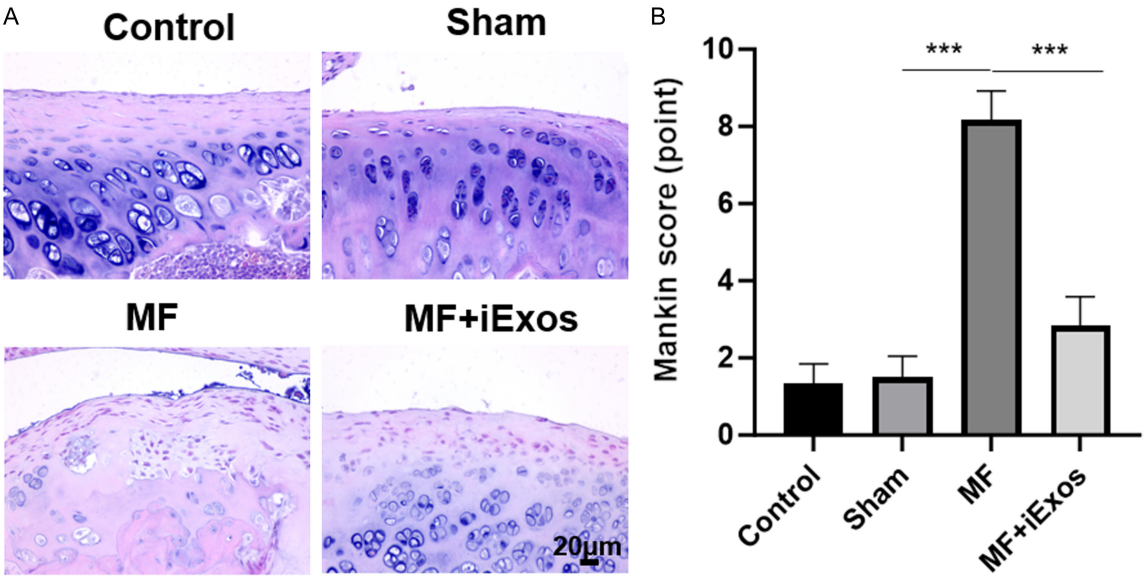


Figure 3. HE staining. A. HE staining images of the four groups. B. Mankin scores of the four groups. ***P<0.001. n=6 per group. Abbreviations: HE, hematoxylin-eosin; MF, microfracture; iExos, induced pluripotent stem cell-derived exosomes.

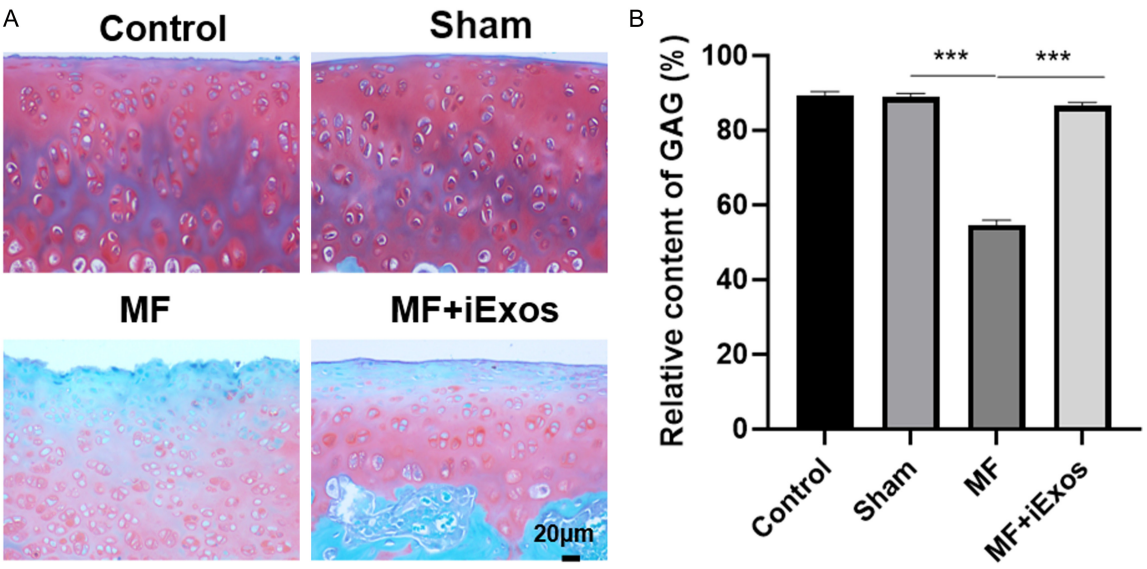


Figure 4. Scarlet O and quin green staining. A. Scarlet O and quin green staining images of the four groups. B. GAG content in the four groups. ***P<0.001. n=6 per group. Abbreviations: GAG, glycosaminoglycan; MF, microfracture; iExos, induced pluripotent stem cell-derived exosomes.

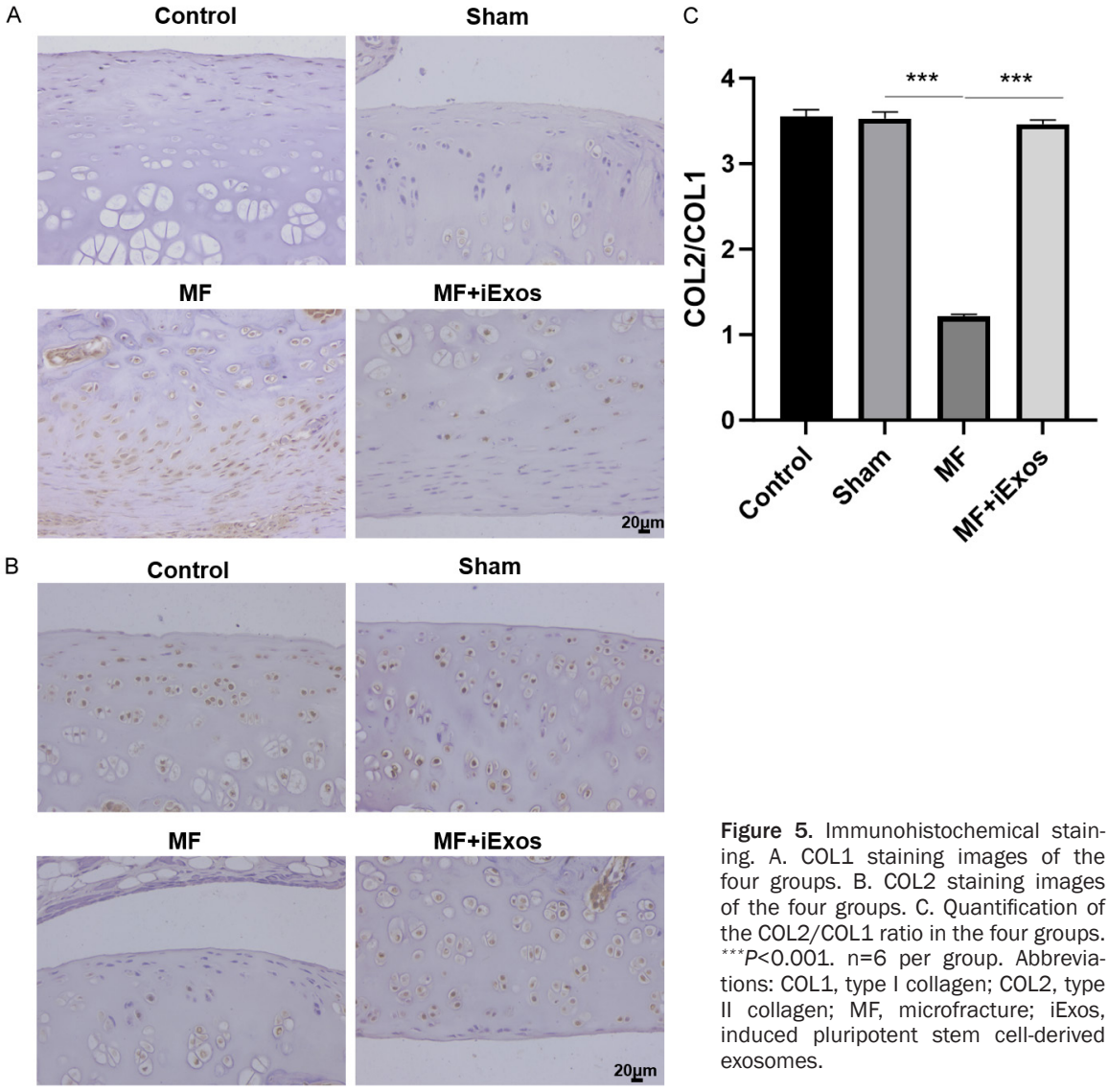


Figure 5. Immunohistochemical staining. A. COL1 staining images of the four groups. B. COL2 staining images of the four groups. C. Quantification of the COL2/COL1 ratio in the four groups. ***P<0.001. n=6 per group. Abbreviations: COL1, type I collagen; COL2, type II collagen; MF, microfracture; iExos, induced pluripotent stem cell-derived exosomes.

thritis-like degenerative changes [21]. iExos treatment upregulated the expression of SOX9, COL2A1 (P<0.05), and ACAN in BMSCs, while it downregulated the expression of COLX, MMP13, and RUNX2 (P<0.05), while the iExos-NC group showed no statistically significant differences in the levels of SOX9, COL2A1, ACAN, COLX, MMP13, and RUNX2 compared to the control group (P>0.05). This result indicated that iExos can effectively guide BMSCs to differentiate into hyaline cartilage and inhibit their hypertrophy process, while the simple exosome carrier (iExos-NC) did not possess such regulatory capabilities. This difference may be due to the fact that the exosomes derived from iPSCs after induction specifically enriched key effector molecules such as miR-140-3p, while the uninduced exosomes lacked such components. Therefore, in this study, exosomes derived from iPSCs after induction were used, which could eliminate non-specific carrier effects and clearly attribute the biological function of iExos to the functional delivery of miR-140-3p, thereby enhancing the reliability of the results and the specificity of mechanism interpretation. Additionally, this effect was reversed after the addition of miR-140-3p inhibitor, suggesting that miR-140-3p is the key effector molecule for iExos to exert the aforementioned regulatory functions. This finding is highly consistent with the recent research results in an osteoar-

thritis model, which also confirmed that miR-140-3p can maintain homeostasis of chondrocytes by targeting HDAC4 [22]. A plausible underlying mechanism is that miR-140-3p exerts its regulatory effects by directly binding to 3'-UTR of HDAC4 or ADAMTS-5 [23, 24]. This interaction subsequently relieves the transcriptional repression of SOX9, thereby promoting its activity. At the same time, it blocks the activation of downstream signaling pathways that drive chondrocyte hypertrophy [23, 24]. Therefore, as a naturally occurring delivery vehicle, iExos can efficiently transport miR-140-3p into BMSCs. This capability provides a precise molecular strategy for optimizing the fate regulation of repair cells following MF surgery. Moreover, given their low immunogenicity and good biocompatibility, iExos hold clear promise for future translation into cell-free therapies.

The recovery of joint function following MF surgery serves as a key clinical indicator for assessing the effectiveness of cartilage repair [25]. Because any repair procedure is to restore pain-free joint mobility and normal activity levels, functional outcome measures are often regarded as more directly relevant than radiographic or histological parameters [25]. In this study, standing time and stride length decreased, whereas joint range of motion score and swing time increased in the MF group compared with the sham group. In the MF+iExos group, standing time and stride length increased compared with the MF group, while joint range of motion score and swing time decreased, suggesting that iExos intervention promotes functional recovery. Gait analysis, is one of the gold-standard methods for evaluating joint function recovery, and the improvement of its results directly reflects the enhancement of the animal's in vivo activity ability [26]. The biomechanical test results of this study showed that the elastic and relaxation modulus of the joint cartilage in MF group were reduced, which is consistent with the characteristic of poor mechanical performance of fibrocartilage [27]; while the two moduli in the MF+iExos group were recovered. The elastic modulus and relaxation modulus are key parameters reflecting the compressive resistance and energy dissipation ability of cartilage, and their recovery to a near-normal level confirms from a biomechanical perspective that iExos promotes the formation of more hyaline cartilage-like repair tissues. A previous investigation has reported that exosomes originating from mesenchymal stem cells can facilitate the repair of cartilage defects [28]. The results obtained are consistent with those observations. The reason may be that iExos regulates the differentiation direction of BMSCs through miR-140-3p, making the new repair tissue rich in COL2 and GAG, thereby being structurally and functionally closer to native cartilage.

Histological assessment is the direct basis for evaluating cartilage repair [29]. In this study, HE staining showed that the repair tissue in the MF group had a rough surface and uneven structure, while the repair tissue in the MF+iExos group was thicker, smoother, and had a more dense cell arrangement. The Mankin score was reduced ($P<0.05$), indicating a reduction in the degree of tissue degeneration. Scarlet O and quin green staining further revealed that the content of GAG in the MF group was decreased, while the GAG content in the MF+iExos group increased, approaching the level of the sham group. GAG is an important component of the extracellular matrix, and its content is closely associated with cartilage integrity and function [30]. Taken together, the above findings regarding tissue morphology and matrix composition preliminarily suggest that treatment with iExos is capable of improving both the structural integrity and the extracellular matrix quality of cartilage repair tissue following MF surgery. This observation is in line with prior histological studies on post-MF repair, which have consistently reported that the tissue regenerated after MF surgery tends to be predominantly fibrocartilaginous in nature, often displaying an irregular surface and only limited deposition of GAGs [31]. Nevertheless, while conventional staining methods such as HE and Safranin O-Fast Green are effective at revealing overall tissue architecture and matrix composition, they fall short of clearly distinguishing the specific phenotypic identity of the repaired tissue. Consequently, accurate phenotypic identification necessitates the incorporation of additional assessments based on collagen type-specific characteristics.

Therefore, this study further examined the levels of COL1 and COL2 in repaired tissues. Immunohistochemical results showed that in MF group, COL1 was highly expressed and COL2 was lowly expressed ($P<0.05$), and the COL2/COL1 ratio was decreased ($P<0.05$), presenting typical features of fibrocartilage; while in the MF+iExos group, COL2 expression was increased, COL1 expression was decreased; the COL2/COL1 ratio was increased, approaching the level of the sham group. The COL2/COL1 ratio is a key indicator for distinguishing hyaline cartilage from fibrocartilage, and the higher the ratio, the closer it is to the native cartilage phenotype [32]. In research on osteoarthritis models, it was also found that after MF surgery, the repair tissue mainly expressed COL1, and it was difficult to form a hyaline cartilage-like structure [33]; while after exosome or growth factor intervention, the expression of COL2 increased, and the repair quality improved [12]. In addition, some scholars have confirmed in the cartilage defect model that overexpression of miR-140-3p can increase the ratio of COL2/COL1 and promote hyaline cartilage-like repair [34]. The possible mechanism is that miR-140-3p can target HDAC4 or ADAMTS-5 to relieve the transcriptional inhibition of SOX9 and block the activation of the downstream hypertrophic signaling pathway, thereby guiding BMSCs to differentiate into hyaline cartilage rather than fibrous cartilage. The immunohistochemical results and histological results are consistent with each other. From the three aspects of morphology, matrix components, and collagen phenotype, they all indicate that iExos intervention improved the quality of cartilage repair tissue after MF surgery, further confirming its promoting effect in hyaline cartilage regeneration.

Based on the results, this research found that iPSCs, under chondrogenic induction conditions, produce iExos rich in miR-140-3p. After these exosomes are taken up by BMSCs, they deliver miR-140-3p, promoting the differentiation of BMSCs towards hyaline cartilage and inhibiting their hypertrophy. When iExos are locally applied after MF surgery, it can optimize the repair microenvironment, ultimately achieving high-quality cartilage repair at the functional, mechanical, histological and molecular levels. Compared with MF alone, the combined treatment with iExos not only enhances the hyaline cartilage characteristics of the repaired tissue, but also avoids the problems of immune rejection and tumor risk that may arise from cell transplantation, demonstrating the unique advantages of the cell-free treatment strategy. Therefore, targeting the iExos-miR-140-3p axis may become an effective intervention strategy for improving the quality of cartilage repair after MF surgery, and thus it has a good clinical translation prospect.

This study has certain limitations. Firstly, although we have provided direct evidence that iExos are enriched with miR-140-3p and deliver it into recipient BMSCs (Supplementary Figure 1A, 1B), the mechanism underlying the selective enrichment of miR-140-3p into iExos during chondrogenic differentiation of iPSCs remains unexplored. Moreover, the possible presence of other synergistic miRNAs or proteins within iExos that may cooperate with miR-140-3p cannot be excluded. Future studies using multi-omics analysis of extracellular vesicles and CRISPR interference techniques are needed to dissect the functional molecular network of iExos. Second, the downstream direct target genes and signaling pathways of miR-140-3p were not fully verified in this study. Although the key role of this miRNA was confirmed by inhibitor experiments, direct evidence such as dual-luciferase reporter assays and target gene manipulation is still lacking, and the mechanistic chain needs further improvement. Third, this study only observed the repair effect at 12 weeks after surgery at the animal level, with no longer-term follow-up data. The risk of long-term degeneration of the repaired tissue cannot be completely ruled out. Future work should include establishing large animal models and performing longer-term follow-up observations to evaluate the safety and efficacy of this strategy.

In conclusion, this study has demonstrated that iExos can promote the chondrogenic differentiation of BMSCs in vitro and inhibit their hypertrophy by delivering miR-140-3p. In vivo, this strategy improves the joint function, biomechanical properties, and quality of the cartilage repair tissue in rats after arthroscopic MF surgery, restoring it to a level close to normal. This strategy provides a new theoretical basis and potential cell-free therapeutic

approach for optimizing repair of cartilage damage after MF surgery.

Disclosure of conflict of interest

None.

Address correspondence to: Drs. Haiming Wang and Chen Chen, Department of Orthopaedic Surgery, Shanghai Sixth People's Hospital, Shanghai, China. E-mail: Wanghaiming189@163.com (HMW); Chenchen9635@126.com (CC)

References

[1] Courties A, Kouki I, Soliman N, Mathieu S and Sellam J. Osteoarthritis year in review 2024: epidemiology and therapy. Osteoarthritis Cartilage 2024; 32: 1397-1404.

[2] Armiento AR, Alini M and Stoddart MJ. Articular fibrocartilage - Why does hyaline cartilage fail to repair? Adv Drug Deliv Rev 2019; 146: 289-305.

[3] Pueyo Moliner A, Ito K, Zaucke F, Kelly DJ, de Ruijter M and Malda J. Restoring articular cartilage: insights from structure, composition and development. Nat Rev Rheumatol 2025; 21: 291-308.

[4] Bumberger A, Homere AJ, Smith RD and Lattermann C. Microfracture and microfracture plus of the knee joint. Clin Sports Med 2025; 44: 513-525.

[5] Seewoonarain S, Ganesh D, Perera E, Popat R, Jones J, Sugand K and Gupte C. Scaffold-associated procedures are superior to microfracture in managing focal cartilage defects in the knee: a systematic review & meta-analysis. Knee 2023; 42: 320-338.

[6] Dhillon J, Decilveo AP, Kraeutler MJ, Belk JW, McCulloch PC and Scillia AJ. Third-generation autologous chondrocyte implantation (cells cultured within collagen membrane) is superior to microfracture for focal chondral defects of the knee joint: systematic review and meta-analysis. Arthroscopy 2022; 38: 2579-2586.

[7] Kalluri R and McAndrews KM. The role of extracellular vesicles in cancer. Cell 2023; 186: 1610-1626.

[8] Cao H, Chen M, Cui X, Liu Y, Liu Y, Deng S, Yuan T, Fan Y, Wang Q and Zhang X. Cell-free osteoarthritis treatment with sustained-release of chondrocyte-targeting exosomes from umbilical cord-derived mesenchymal stem cells to rejuvenate aging chondrocytes. ACS Nano 2023; 17: 13358-13376.

[9] Ferreira MJS, Mancini FE, Humphreys PA, Ogene L, Buckley M, Domingos MAN and Kimber SJ. Pluripotent stem cells for skeletal tissue engineering. Crit Rev Biotechnol 2022; 42: 774-793.

[10] Al-Modawi RN, Brinchmann JE and Karlsen TA. Extensive downregulation of immune gene expression by microRNA-140-3p 5' isomiR in an in vitro model of osteoarthritis. Osteoarthr Cartil Open 2021; 3: 100189.

[11] Wang N, Liu X, Tang Z, Wei X, Dong H, Liu Y, Wu H, Wu Z, Li X, Ma X and Guo Z. Increased BMSC exosomal miR-140-3p alleviates bone degradation and promotes bone restoration by targeting Plxnb1 in diabetic rats. J Nanobiotechnology 2022; 20: 97.

[12] Zhang S, Chu WC, Lai RC, Lim SK, Hui JH and Toh WS. Exosomes derived from human embryonic mesenchymal stem cells promote osteochondral regeneration. Osteoarthritis Cartilage 2016; 24: 2135-2140.

[13] Kara H, Çağlar C, Asiltürk M, Karahan S and Uğurlu M. Comparison of a manual walking platform and the CatWalk gait analysis system in a rat osteoarthritis model. Adv Clin Exp Med 2021; 30: 949-956.

[14] Puhakka J, Paatela T, Salonius E, Muhonen V, Meller A, Vasara A, Kautiainen H, Kosola J and Kiviranta I. Enhancing the reliability of cartilage repair evaluation: a simplified volume-based approach. J Orthop Res 2025; 43: 1387-1395.

[15] Abughazaleh N, Seerattan RA, Hart DA, Reimer RA and Herzog W. A novel Osteoarthritis scoring system to separate typical OA joint degeneration from non-typical lesions in male Sprague Dawley rats. Osteoarthr Cartil Open 2024; 6: 100521.

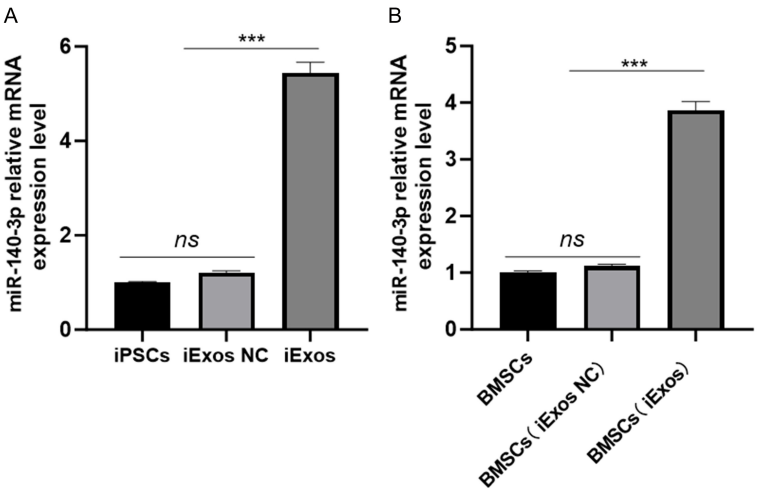
[16] Pałka K, Kubisa M, Akbas A, Kubisa M and Dobrakowski M. Does scaffold enhancement show significant superiority over microfracture alone for treating knee chondral defects? A systematic review and meta-analysis of randomised clinical trials. Knee Surg Sports Traumatol Arthrosc 2025; 33: 2027-2043.

[17] Wen HJ, Yuan LB, Tan HB and Xu YQ. Microfracture versus enhanced microfracture techniques in knee cartilage restoration: a systematic review and meta-analysis. J Knee Surg 2022; 35: 707-717.

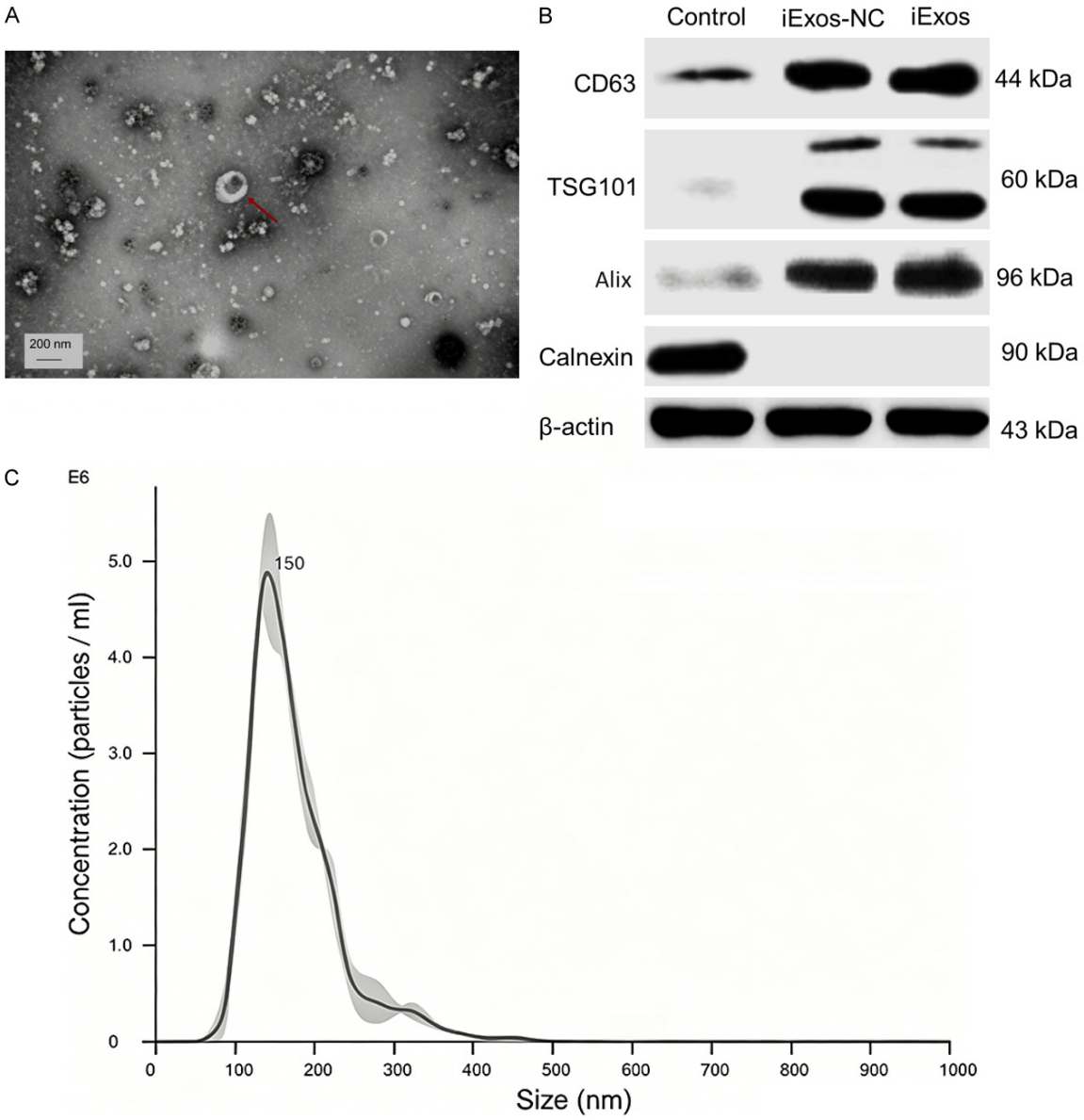
[18] Hu Y, Cheng P, Jia L, Hao X, Ding G, Han M, Fan J, Lu W, Zhou C, Luo Z and Yang L. Extracellular vesicles originating from induced pluripotent stem cell-derived chondrocytes facilitate the regeneration of osteoarthritic cartilage. J Orthop Translat 2026; 56: 101035.

[19] Jia Y, Xie L, Tang Z, Wang D, Hu Y, Zhang G, Chen Y and Gao Q. Parathyroid hormone promotes cartilage healing after free reduction of mandibular condylar fractures by upregulating Sox9. Exp Biol Med (Maywood) 2021; 246: 2249-2258.

[20] Lefebvre V, Angelozzi M and Haseeb A. SOX9 in cartilage development and disease. Curr Opin Cell Biol 2019; 61: 39-47.
[21] Ruiz-Fernández C, González-Rodríguez M, Abella V, Francisco V, Cordero-Barreal A, Ait Eldjoudi D, Farrag Y, Pino J, Conde-Aranda J, González-Gay MÁ, Mera A, Mobasheri A, García-Caballero L, Gándara-Cortés M, Lago F, Scotece M and Gualillo O. WISP-2 modulates the induction of inflammatory mediators and cartilage catabolism in chondrocytes. Lab Invest 2022; 102: 989-999.
[22] Hu Y, Liu HX, Xu D, Xue X and Xu X. The anti-inflammatory effect of miR-140-3p in BMSCs-exosomes on osteoarthritis. Acta Chir Orthop Traumatol Cech 2023; 90: 267-276.
[23] Woods S, Charlton S, Cheung K, Hao Y, Soul J, Reynard LN, Crowe N, Swingler TE, Skelton AJ, Piróg KA, Miles CG, Tsompani D, Jackson RM, Dalmay T, Clark IM, Barter MJ and Young DA. microRNA-seq of cartilage reveals an overabundance of miR-140-3p which contains functional isomiRs. RNA 2020; 26: 1575-1588.
[24] Ren T, Wei P, Song Q, Ye Z, Wang Y and Huang L. MiR-140-3p ameliorates the progression of osteoarthritis via targeting CXCR4. Biol Pharm Bull 2020; 43: 810-816.
[25] Byun J, Jung M, Chung K, Moon HS, Jung SH, Kim JK and Kim SH. Comparison of magnetic resonance observation of cartilage repair tissue score and functional outcomes between microdrilling and microfracture for cartilage lesions of distal femur: a retrospective comparative study. Cartilage 2025; 19476035251360504.
[26] Takenouchi S, Minato T, Fukuda M, Kobayashi K and Murata T. Development of a quantitative gait analysis in an osteoarthritis rat model using machine learning. J Pharmacol Sci 2026; 160: 59-63.
[27] Liao L, Gu F, Xiong F, Pan X, Zhao G and Mi J. Biomechanical analysis of transosseous repair versus combined transosseous with capsular repair for triangular fibrocartilage complex tears with instability. J Hand Surg Am 2025; 50: 752.e751-752.e758.
[28] Xie Y, Liu Q, Tan J, Lu Y, Li Y, Ye H, Xu Z, Wang M, Wang C, Li X, Xue J and Yan Y. CAP-CD56(+) CD271(+) BMSCs exos-loaded PVA/SA sustained-release hydrogel attenuates chondrocyte senescence and ameliorates lumbar facet joint osteoarthritis. Bioact Mater 2026; 57: 73-92.
[29] Houtman E, van Hoolwerff M, Lakenberg N, Suchiman EHD, van der Linden-van der Zwaag E, Nelissen RGHH, Ramos YFM and Meulenbelt I. Human osteochondral explants: reliable biomimetic models to investigate disease mechanisms and develop personalized treatments for osteoarthritis. Rheumatol Ther 2021; 8: 499-515.
[30] Maeda T, Kuriyama S, Yoshida S, Nishitani K, Nakamura S and Matsuda S. Decreased elastic modulus of knee articular cartilage based on new macroscopic methods accurately represents early histological findings of degeneration. Cartilage 2024; 15: 461-470.
[31] Jarecki J, Waśko MK, Widuchowski W, Tomczyk-Warunek A, Wójciak M, Sowa I and Blicharski T. Knee cartilage lesion management-current trends in clinical practice. J Clin Med 2023; 12: 6434.
[32] Bielajew BJ, Hu JC and Athanasiou KA. Methodology to quantify collagen subtypes and crosslinks: application in minipig cartilages. Cartilage 2021; 13: 1742S-1754S.
[33] Meng J, Lu J, Jiang C, Deng L, Xiao M, Feng J, Ren T, Qin Q, Guo S, Wang H, Yao J and Li J. Collagen hydrogel-driven pyroptosis suppression and combined microfracture technique delay osteoarthritis progression. Biomaterials 2025; 314: 122817.
[34] Bao C and He C. The role and therapeutic potential of MSC-derived exosomes in osteoarthritis. Arch Biochem Biophys 2021; 710: 109002.



Supplementary Figure 1. qRT-PCR validation of miR-140-3p enrichment and delivery. A. miR-140-3p levels in iExos, iExos-NC, and parental iPSCs. ***P<0.001 vs. iPSCs and iExos-NC. B. miR-140-3p levels in BMSCs after co-culture with PBS, iExos-NC, or iExos. ***P<0.001 vs. control and iExos-NC. ns, P>0.05. Each group: n=3. Abbreviations: qRT-PCR, quantitative reverse transcription polymerase chain reaction; miR/mRNA, microRNA; iPSCs, induced pluripotent stem cells; iExos, iPSC-derived exosomes; iExos-NC, exosomes from non-induced iPSCs; BMSCs, bone marrow mesenchymal stem cells; PBS, phosphate-buffered saline.



Supplementary Figure 2. Exosome identification. A. Transmission electron microscopy image, with red arrows indicating exosomes. B. Protein expression of CD63, TSG101, Alix, calnexin, and β-actin. C. Nanoparticle tracking analysis. Abbreviations: CD63, cluster of differentiation 63; TSG101, tumor susceptibility gene 101 protein; Alix, ALG-2-interacting protein X; β-actin, beta-actin; iExos, induced pluripotent stem cell-derived exosomes; iExos-NC, exosomes from non-induced induced pluripotent stem cells.